

A NEW HETEROCYCLIC COMPOUND: CRYSTAL STRUCTURE AND ANTICANCER ACTIVITY AGAINST HUMAN LUNG ADENOCARCINOMA CELLS

E.-H. Shi¹, L.-R. Wang¹, S. Zhao¹, L. Shen¹,
C.-Y. Zhang¹, X.-X. Li¹, H. Li², and D.-L. Zhang^{1*}

New heterocyclic compound (S)-3-(4-(5-bromo-2-chlorobenzyl)phenoxy)tetrahydrofuran (**1**), designed by utilizing 5-bromo-2-chlorobenzoic acid (**2**) as the starting material, is obtained by the organic synthesis and then characterized by single crystal X-ray crystallography, ¹H NMR and IR spectroscopy. In the biological study, the CCK-8 assay is performed to evaluate the inhibitory effect of the compound on SPC-A-1 human lung adenocarcinoma cells in vitro by measuring the cancer cell viability. Then, the anticancer activity of the compound is also confirmed by the in vivo xenograft experiment by measuring the mice body weight and the cancer volume.

DOI: 10.1134/S0022476620070215

Keywords: heterocycles, X-ray, anticancer, molecular docking, lung adenocarcinoma.

INTRODUCTION

One of the leading causes of death worldwide is cancer [1-3]. The World Bank income groups stated that from 2008 to 2030, 12.7 million cancer case incidences will increase to 21.4 million [4, 5]. In spite of enormous efforts to generate available chemotherapy drugs, significant toxicity and selectivity problems remain. The resistance of cancer cells to anticancer agents and the modern chemotherapy toxicity stimulates us to look for novel therapies and prevention approaches of the potential disease [6].

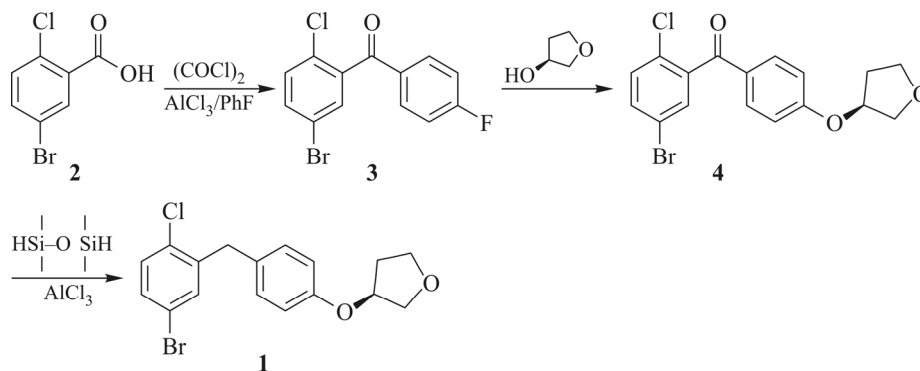
Empagliflozin is a medicinally crucial aryl glycoside used in the therapy of type 2 diabetes [7]. In the synthesis of empagliflozin, (S)-3-(4-(5-bromo-2-chlorobenzyl)phenoxy)tetrahydrofuran (**1**) is one of the most crucial intermediates [8, 9]. Hence, substantial attention has been paid to the synthesis, crystal configuration and characterization of compound **1**, which have not been reported previously.

This work describes the characterization and synthesis of title compound **1**. Compound **1** was designed by the use of 5-bromo-2-chlorobenzoic acid (**2**) as the starting material yielding (5-bromo-2-chlorophenyl)(4-fluorophenyl) methanone (**3**). It reacted with (S)-tetrahydrofuran-3-ol to produce (S)-(5-bromo-2-chlorophenyl)(4-((tetrahydrofuran-3-yl)oxy)phenyl)methanone (**4**). We obtained title compound **1** after the reduction of compound **4** with 1,1,3,3-tetramethyldisiloxane (Scheme 1). Furthermore, the inhibitory effect and cytotoxicity of the compound on SPC-A-1 human lung adenocarcinoma cells were

¹Medical Oncology, Heilongjiang Province Hospital, Harbin, Heilongjiang, P. R. China; *dongli_zhang11@126.com.

²Department of Orthopedics, Zhejiang University, Yiwu, Zhejiang, P. R. China. Original article submitted August 12, 2019; revised October 22, 2019; accepted November 22, 2019.

evaluated by the CCK-8 assay. The results indicated the excellent antitumor activity of the compound in vitro by reducing the cancer cell viability. Then, in vivo xenograft experiments were conducted to explore the effect of the compound on SPC-A-1 human lung adenocarcinoma cells. The results also indicated the antitumor activity against SPC-A-1 cells in vivo.



Scheme 1. Synthesis route of compound **1**.

EXPERIMENTAL

Apparatus and materials. We utilized the Bruker Equinox-55 spectrophotometer to acquire the IR spectra. We measured the ^1H NMR spectra on the Varian Inova-400 spectrometer at 400 MHz. The mass spectra were recorded on a micrOTOF-Q II mass spectrometer. The melting points were measured on the XT-4 micro melting device, and the thermometer was not corrected.

Characterization and synthesis of compounds 1, 3, and 4. With regard to a slurry **2** (0.0354 mol, 8.34 g), to a catalytic amount of DMF (0.7 mmol, 0.055 mL) along with fluorobenzene (50 mL) oxalyl chloride (0.0372 mol, 3.24 mL) was added dropwise. Then we stirred it for two hours at 21–25 °C, and concentrated to a low volume (30 mL). An additional amount of fluorobenzene (20 mL) was added. Then we cooled the solution to 0–5 °C. We added AlCl_3 to this solution in three portions (5.19 g, 0.0389 mol), keeping the internal temperature <25 °C. We gathered the solids through filtration, and then dried them in an oven to obtain compound **3** as white crystals (10.77 g, 96.94%). ^1H NMR under 400 MHz (CDCl_3) δ : 7.19–7.13 (m, 2H), 7.34 (d, 1H), 7.50 (d, 1H), 7.57 (dd, 1H), 7.83–7.81 (m, 2H).

1 M potassium *tert*-butoxide (0.0370 mol, 3.7 mL) was added dropwise to the mixture of compound **3** (0.0336 mol, 10.54 g) with (S)-tetrahydrofuran-3-ol (0.0336 mol, 2.96 g) in THF (36 mL). Then we stirred this mixture for 30 min at 7–10 °C, and quenched it with water (35 mL). MTBE (35 mL) was added to the residue. Then all the layers were parted. The whole organic was vacuum concentrated. IPA (25 mL) and water (2.3 mL) were added to the residue at 60 °C for 60 min, and the slurry was gradually cooled to 0–5 °C. We gathered the solids through filtration and then dried them in an oven to obtain compound **4** as white crystals (10.93 g, 85.19%). ^1H NMR under 400 MHz (CDCl_3) δ : 2.19–2.12 (m, 1H), 2.31–2.20 (m, 1H), 3.94–3.89 (m, 1H), 4.05–3.97 (m, 3H), 5.01 (m, 1H), 6.91 (d, 2H), 7.32 (d, 1H), 7.48 (d, 1H), 7.54 (dd, 1H), 7.76 (d, 2H).

The solution of compound **4** (0.0231 mol, 8.81 g) with AlCl_3 (0.0463 mol, 6.17 g) in toluene (45 mL) was supplemented with 1,1,3,3-tetramethyldisiloxane (4.04 g, 0.0301 mol) at <20 °C. We stirred this mixture for 1.5 h at 20–23 °C. Then we cooled this mixture to 0–5 °C, supplemented it with ice water (40 mL) for 15 min, and separated the layers. The residue was supplemented with acetonitrile (40 mL) and water (20 mL). We cooled the resulting mixture to 0–3 °C and stirred for 2 h. The solids were collected by filtration and dried in an oven to give **1** as white crystals (7.75 g, 91.28%). ^1H NMR under 400 MHz (CDCl_3) δ : 2.19–2.12 (m, 1H), 2.31–2.20 (m, 1H), 3.94–3.89 (m, 1H), 4.05–3.97 (m, 3H), 5.01 (m, 1H), 6.91 (d, 2H), 7.32 (d, 1H), 7.48 (d, 1H), 7.54 (dd, 1H), 7.76 (d, 2H). HRMS (ESI⁺), m/z : calcd for $\text{C}_{17}\text{H}_{16}\text{BrClO}_2$ 388.9920 [$\text{M}+\text{Na}^+$]; found 388.9939.

Crystal structure solution. A proper single crystal of compound **1** obtained by slow volatilization of its CH₂Cl₂ solution was discreetly chosen under an optical microscope. Then we glued the single crystal on the thin glass fiber. The intensity data on compound **1** were gathered on an Oxford Xcalibur E diffractometer. Empirical absorption corrections of these data were applied utilizing the SADABS system [10]. The configuration was figured out through a direct approach. By virtue of the SHELXS-97 program we refined the data through the full-matrix least-squares approach on F^2 . All non-hydrogen atoms of compound **1** were refined as anisotropic, and all hydrogen atoms bonded to carbon atoms were fixed at their perfect positions. Table 1 summarizes the structural refinement results and crystal data for compound **1**.

Cell Counting Kit-8 assays. The viability of SPC-A-1 human lung adenocarcinoma cells after treating by the compound was detected according to the manufacturer instructions with the Cell Counting Kit-8 (CCK-8, Beyotime Biotechnology, China) [11]. In brief, the SPC-A-1 cells in the logarithmic growth phase were collected and seeded into 96-well plates to the final density of $5 \cdot 10^3$ cells/well. Then, the cells were incubated at 37 °C, 5% CO₂ in an incubator for the cell growth to the 70-80% confluence. Next, the compound at serious dilutions (from 1 µg/mL to 80 µg/mL) was added into wells for 24 h cell treatment for incubation. After treatment, the 10 µL CCK-8 solution was added, and the absorbance levels for each well was measured using a microplate reader (Bio-Tek, USA). The effect of the compound on normal human cells ESBA-2B was also evaluated by the CCK-8 assay, as described above. Each group contains triplicate wells, and this experiment was repeated at least three times.

Xenograft tumor model. For the xenograft experiment, BALB/c nude mice (male, 5-6 weeks) were purchased from Model animal research center of Nanjing University. All mice were housed in a specific pathogen-free environment under the guidelines for the laboratory animal care [12]. All the animal experiments were approved by the Institutional of Animal Care and Use Committee of China. For the xenograft experiment, $5 \cdot 10^6$ SPC-A-1 human lung adenocarcinoma cells in the logarithmic growth phase were collected in 100 µL of the PBS solution and then inoculated in the subcutaneous tissue of the nude mice. The mice were randomized into three groups on the 10th day after cancer cell implantation; the compound was injected at 2 mg/kg and 5 mg/kg for antitumor treatment. 5% DMSO was used as the negative control for the control group treatment. The tumor volume was measured every 3 days for 15 days and calculated using the following formula: (length×width²). The mice weight was recorded at the end of the experiment.

TABLE 1. Structure Refinement and Crystal Data for Compound **1**

Parameter	1
Formula	C ₁₇ H ₁₆ BrClO ₂
M_r	367.66
Crystal system	Monoclinic
Space group	C2
$a, b, c, \text{Å}$	21.608(3), 6.2115(4), 15.954(2)
β, deg	132.94(2)
$V, \text{Å}^3$	1567.6(5)
Z	4
Crystal size, mm	0.32×0.26×0.2
$D_{\text{calc}}, \text{g/cm}^{-3}$	1.558
$\mu(\text{MoK}\alpha), \text{mm}^{-1}$	2.794
θ range, deg	1.885 to 25.348
Reflections collected	5284
No. unique data ($R(\text{int})$)	2814 (0.0254)
No. data with $I \geq 2\sigma(I)$	2423
$R_1 / wR_2(\text{all data})$	0.0349 / 0.0770
CCDC	1866596

Simulation details. Through the use of a B3LYP/6-31G(*d*) basis set, the configuration of compound **1** was optimized by DFT. The energy calculations as well as the configuration optimization were carried out using the GAUSSIAN 09 program.

Autodock Vina v1.2 has been applied to investigate the binding mode of compound **1** with tubulin. Tubulin was used as downloaded and has no further modification from the protein data bank. The geometry configurations of compounds A and B were optimized by quantum chemistry calculations using Gaussian 09 at the B3LYP level of theory with the 6-31G* basis set. We utilized AutoDockTools v1.5.6 to transmit the optimized configurations of compounds A and B and 1AS0 to AutoDock vina input files. Only polar hydrogen atoms were taken into account in the configurations. The central coordinates of the microtubule search grid were set as (38.15, -26.99, 6.18) and the search grid length was 15. If not particularly mentioned, all parameters required by AutoDock vina were applied as default. Through PyMoL v1.8.6, we could visualize and analyze the results.

RESULTS AND DISCUSSION

Molecular structure. Through the single crystal X-ray diffraction analysis, we could identify the configuration of compound **1** (C₁₇H₁₆BrClO₂). The relevant result indicates that compound **1** has the monoclinic crystal system and the space group is *C*2. The compound exhibits a three-dimensional supramolecular structure organized by two types hydrogen bonds such as C–H···Cl and C–H···O. The molecular structural unit of compound **1** is shown in Fig. 1. Within the structure, the dihedral angle of the adjacent two six-membered rings (C(5)–C(10) and C(12)–C(17)) is 87.49°. The C–Br, C–Cl, C–O, and C–C bond lengths are 1.899(6) Å, 1.737(6) Å, 1.373(7)–1.430(8) Å, and 1.371(9)–1.525(9) Å, respectively. All the above-mentioned bond distances in this compound fall in their normal ranges.

Moreover, the two types of hydrogen bonds, including C–H···O and C–H···Cl, could be discovered in its packing structure. Table 2 provided the particular information on the hydrogen bonding.

By the two types of hydrogen bonds, a three-dimensional supramolecular network is generated. Fig. 2 shows the crystal packing configuration of the compound along the *b* axis. The hydrogen bonds play important roles for the stability of the structure.

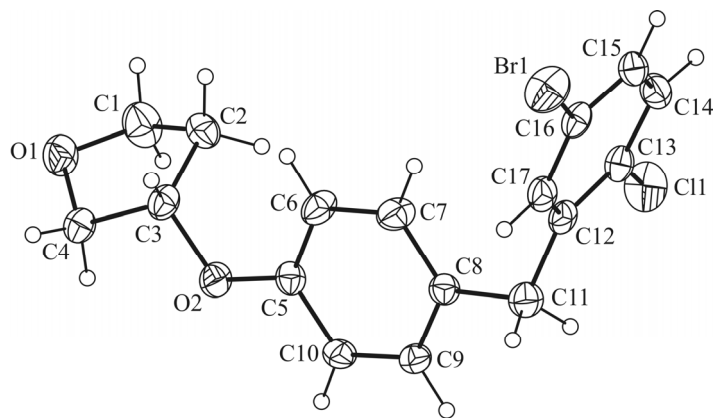


Fig. 1. Molecular structural unit of compound **1**.

TABLE 2. Hydrogen Bonds (Å) in Compound **1**

D–H...A	D–H	H...A	D...A	D–H...A	Symmetry code
C11–H11B...Cl1	0.9700	2.7100	3.068(7)	103.00	3/2– <i>x</i> , 1/2+ <i>y</i> , 1– <i>z</i>
C17–H17...O1	0.9300	2.4700	3.342(8)	155.00	

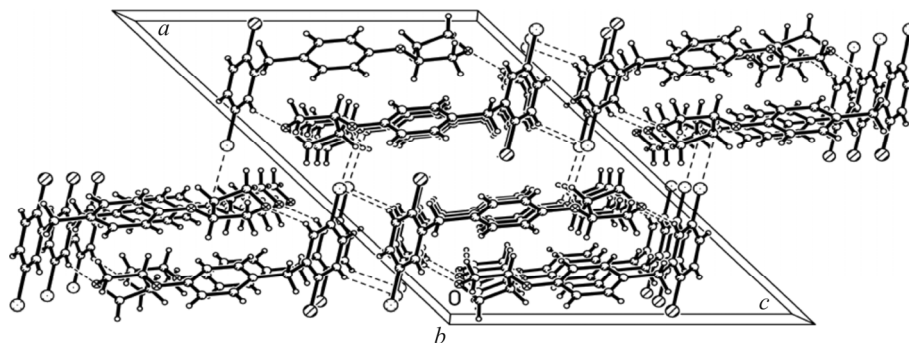


Fig. 2. Crystal packing of compound **1** along the *b* axis.

Compound inhibits only the cancer cell viability rather than normal cells. After the successful design and synthesis of the compound with a totally novel structure, the anticancer activity of this compound was evaluated by the CCK-8 assay. The cancer and normal cells were incubated with various concentrations of the compound ranging from 1 μM to 100 μM for 24 h. As the results show (Fig. 3), the viability of SPC-A-1 human lung adenocarcinoma cells was significantly reduced in a dose-dependent manner (*a*), but the compound showed no influence on the viability of normal cells (*b*), which indicated that the compound has an excellent anticancer activity with a high selectivity and a minor side effect.

In vivo antitumor activity of the compound. In the previous study, we have confirmed the anticancer activity of the compound *in vitro*. To further explore the anticancer capability of the compound *in vivo*, the xenograft tumor model was constructed by injecting SPC-A-1 human lung adenocarcinoma cells, followed by treating with the compound at dosages of 2 mg/kg and 5 mg/kg. At the end of this treatment, we can see the results illustrated in Fig. 4*a*. The tumor volume of the group treated with the compound was about $283.33 \pm 46.67 \text{ mm}^3$ (5 mg/kg), which was significantly smaller than that of the control group ($1500.000 \pm 173.21 \text{ mm}^3$). Moreover, the average weights of tumors in the group treated with the compound were $0.69 \pm 0.041 \text{ g}$ and $0.25 \pm 0.063 \text{ g}$ (2 mg/kg and 5 mg/kg), which were significantly lower than those in the control group (Fig. 4*b*). These results indicated that the compound could inhibit the xenograft tumor growth in nude mice.

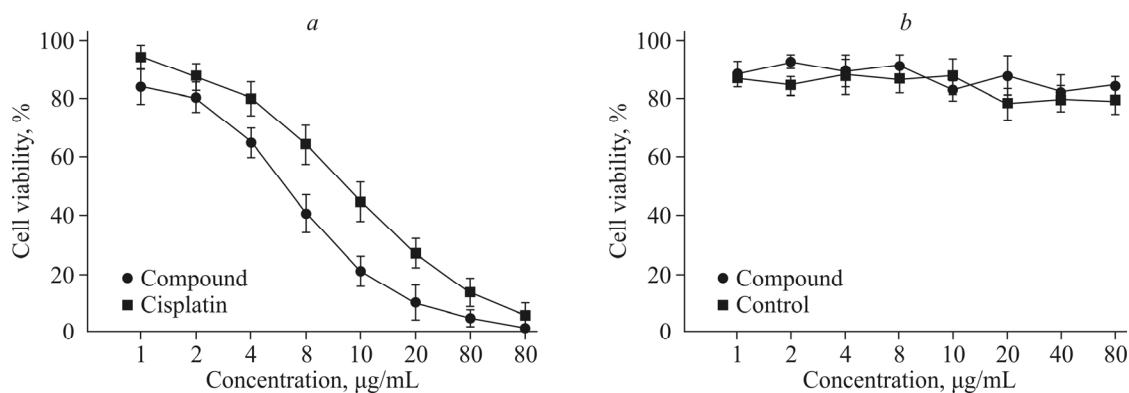


Fig. 3. Inhibited SPC-A-1 human lung adenocarcinoma cell viability after treating with the compound. SPC-A-1 cells were exposed to the compound at various concentrations (1 $\mu\text{g/mL}$, 2 $\mu\text{g/mL}$, 4 $\mu\text{g/mL}$, 8 $\mu\text{g/mL}$, 10 $\mu\text{g/mL}$, 20 $\mu\text{g/mL}$, 40 $\mu\text{g/mL}$, 80 $\mu\text{g/mL}$) for 24 h. The cell viability curves were plotted by the CCK8 assay (*a*). The cytotoxicity of the compound on BEAS-2B cells was measured by the CCK-8 assay (*b*). All experiments were performed in triplicate.

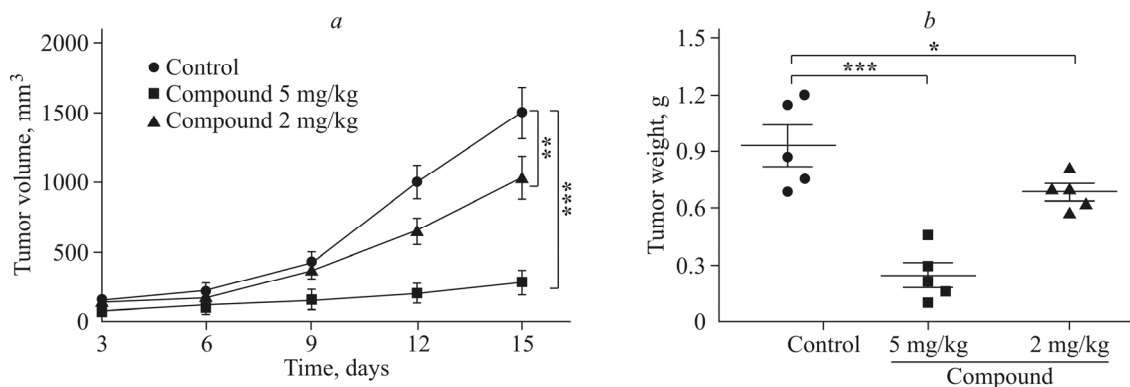


Fig. 4. Reduced tumor volume and tumor weight in the xenograft model after treating with the compound. The SPC-A-1 human lung adenocarcinoma cells were injected into nude mice to construct the xenograft model, and the compound was given at 2 mg/kg and 5 mg/kg for treatment. The average tumor volumes of xenografts in nude mice after treatment with the compound (a); the average weight of tumors at the end of this treatment (b).

TABLE 3. Comparison of the Simulated and Experimental Structural Parameters of the Selected Bond Angles, Bond Lengths and Torsion Angles of Compound **1**

Parameter	X-ray	Calculation
Bond length, Å		
C1–O1	1.420	1.418
C4–O1	1.394	1.419
C3–O2	1.430	1.426
C5–O2	1.373	1.361
C13–C11	1.737	1.751
C16–Br1	1.899	1.907
Torsion Angles, deg		
C1–O1–C4	105.6	108.9
C3–O2–C5	118.3	120.7
C8–C11–C12	116.6	114.7
O1–C4–C3–O2	–139.6	–106.9
C2–C3–O2–C5	73.9	80.8
C8–C11–C12–C13	–85.3	–76.6

Molecular docking. The computer simulation has become more and more popular in assisting and explaining the experimental phenomenon. Here the density functional theory and molecular docking methods have been performed to study the geometry parameters of compound **1** and the potential usage when interacting with protein. Before the molecular docking has been carried out, the molecular structure of compound **1** taken from the X-ray measurement was optimized at the B3LYP/DEF2-SVP level of theory, after which the global minimum of the molecular structure could be found and compared with the experimental results (Table 3). From the table we can see that the maximum discrepancies for bonds, bond and torsion angles are 0.025 nm, 3.3 deg and 32.0 deg, respectively, which are in good agreement with those of the X-ray diffraction experiment.

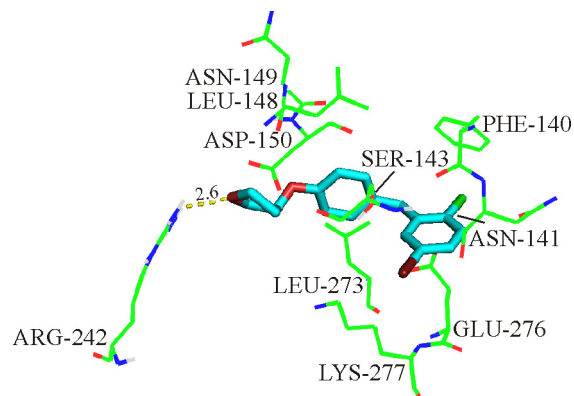


Fig. 5. Most favorable binding mode between compound **1** (stick) and environmental residues which from protein 1AS0, residue labels, the polar interaction as well as its length are shown explicitly.

Then the molecular docking has been performed. The molecular structure used in the autodocking simulation is from the DFT calculation. From the autodocking simulation we found nine possible binding modes between compound **1** and the test protein 1AS0, in which the most stable binding mode is displayed in Fig. 5. The corresponding affinity binding energy is -7.8 kcal/mol, and the polar mutual effect length is 2.6 Å, which indicates a strong hydrogen bond. As depicted in Fig. 5, the most stable binding mode is formed between the oxygen atoms on the five-membered ring and the ARG-242 residue from the protein, while the other polar atoms such as Cl and Br on the phenyl ring do not have any polar mutual effects with environmental residues ASN-149, ASP-150, LEU-148, SER-143, and so on.

CONCLUSIONS

In summary, a new heterocyclic compound was synthesized and characterized by single crystal X-ray diffraction, HRMS, ^1H NMR, and IR spectroscopy. In the biological study, we aimed at exploring candidates for the cancer treatment. Firstly, CCK-8 was performed to evaluate the inhibitory effect of the compound on SPC-A-1 human lung adenocarcinoma cells, and the results indicated the excellent antitumor activity of the compound in vitro. Then the anticancer activity of the compound was also confirmed in the in vivo xenograft experiment.

FUNDING

This work was supported by grants from the scientific research project of Heilongjiang health and Family Planning Commission (2018-267).

CONFLICT OF INTERESTS

The authors declare that they have no conflict of interests.

REFERENCES

1. E. A. Rauscher, M. Dean, G. Campbell-Salome, and J. B. Barbour. *Soc. Sci. Med.*, **2019**, *242*, 112592.
2. S. Ozdemir, C. Malhotra, I. Teo, G. M. Yang, R. Kanavaran, A. C. Yee, and E. A. Finkelstein. *Ann. Acad. Med. Singapore*, **2019**, *48*, 241.
3. A. C. Raymond, B. Gao, L. Girard, J. D. Minna, and D. Gomika Udugamasooriya. *Sci. Rep.*, **2019**, *9*, 14954.

4. S. Saedmocheshi, M. Saghebjo, Z. Vahabzadeh, and D. Sheikholeslami-Vatani. *Med. Sci. Sports Exercise*, **2019**, *51*, 2210.
5. B. Yang, H. Ji, Y. Ge, S. Chen, H. Zhu, and G. Lu. *Front. Oncol.*, **2019**, *9*, 908.
6. Z. H. Zhang, Z. Y. Luan, F. Han, H. Q. Chen, W. B. Liu, J. Y. Liu, and J. Cao. *Oncol. Lett.*, **2019**, *18*, 5523.
7. R. Assaly, D. Gorny, S. Compagnie, E. Mayoux, J. Bernabe, L. Alexandre, F. Giuliano, and D. Behr-Roussel. *J. Sex. Med.*, **2018**, *15*, 1224.
8. A. J. Scheen. *Expert Opin. Drug Saf.*, **2018**, *17*, 837.
9. E. Hoch, J. C. Florez, E. S. Lander, and S. B. R. Jacobs. *Cell Rep.*, **2019**, *29*, 778.
10. G. M. Sheldrick. SHELXL-97, Program for Solution Crystal Structure and Refinement. University of Göttingen: Germany, **1997**.
11. Z. Zhong, F. Zhou, D. Wang, M. Wu, W. Zhou, Y. Zou, J. Li, L. Wu, and X. Yin. *Oncol. Rep.*, **2018**, *40*, 3852.
12. S. Wang, C. Zhang, Y. Li, P. Li, D. Zhang, and C. Li. *Cancer Chemother. Pharmacol.*, **2019**, *83*, 519.